

<https://doi.org/10.1038/s43247-024-01265-2>

Complete transition from mantle plume to mantle exhumation on the Central Atlantic Guyana/Suriname margin

Check for updates

Bill Kilsdonk¹ ✉, James Trude¹, Tim Grow¹, Bryan Ott^{1,3} & Gianreto Manatschal²

Modern data are clarifying tectonic transitions from continents to oceans. The importance of magmatic additions relative to mechanical extension varies between cases and through time based on observations of isolated margins and ridges. Magma poor spreading centers and magma rich continental margins are both well known. Here we present data to document the complete and continuous evolution from a magma rich Central Atlantic margin to a magma-starved ocean floor. Tectonic changes correlate with separation rate changes. Early Jurassic hotspot volcanism initially overwhelmed slow extension to build the Demerara Plateau at the eastern edge of the margin, but hotspot activity waned near the end of the Middle Jurassic. Normal spreading rates and normal thickness oceanic crust prevailed through most of the Oxfordian. Spreading slowed in the Kimmeridgian but magmatic addition slowed even more, evidenced by normal faults that offset the full oceanic crust and by outboard exhumed mantle.

The Guyana/Suriname margin, offshore northern South America (Fig. 1), formed during the Jurassic opening of the Central Atlantic and is delimited by one active and three ancient tectonic boundaries^{1–6}. The Demerara Plateau, immediately east of the landward limit of ocean crust (LALOC in Fig. 1b), is a 25 km to 30 km thick magmatic succession of basalt flows (Fig. 2a) that dip gently to the northwest in a sequence of Seaward Dipping Reflectors (SDRs)^{1,2,6}. The active Barbados accretionary prism forms the northwestern boundary of the margin. To the northeast, Jurassic seafloor abuts Cretaceous oceanic crust across a northwest-southeast trending margin that began as an Aptian-Albian transpressional oceanic transform but became an oblique divergent plate boundary in the mid-Aptian^{4,7}. Axes of compressional structures parallel this outer northwest-southeast trending boundary⁴. The southwestern boundary was a zone of highly oblique continental extension between the Florida Block and South America during the early to mid-Jurassic. It evolved to an ocean-continent transform during the mid-Jurassic. NW-SE continental extension of the margin gave way first to oceanic accretion with plate motion parallel to the transform margin in the Callovian, and later to oceanic extension in the same direction. Because the Florida Block is coupled to the North American plate, and present-day South America was part of Gondwana throughout the Jurassic, relative motions between North America and Gondwana^{3,7,8} define both the relative motion across the Jurassic transform margin and the roughly orthogonal translation of the Florida block away from the Demerara Plateau. Plate scale

transform motion ceased in the wake of the northwest migrating spreading center, leaving ocean-continent boundaries that passively juxtapose continental crust with seafloor of varying composition⁸.

Continental margins have been described as either magma-rich or magma-poor^{9,10} following a similar bipartite division of seafloor created during plate separation^{11,12}. It is now clear that modes of seafloor spreading vary with spreading rate, tectonic position relative to ridge-transform intersections^{13–19}, and with regional plate kinematic history²⁰. Spreading rate appears to be a primary control^{14,21,22}. Slow (<4 cm/yr) and ultraslow (<2 cm/yr) ridges tend to be magma poor, although mantle plume related magmatism is also a factor²³. Mixed modes occur on slow and ultra-slow spreading ocean ridges where inside corners of ridge-transform intersections are magma poor, accommodated by faults leading to “inside corner massifs” or oceanic core complexes. Concurrent separation at opposing outside corners may involve magmatic addition^{13,15–18}.

Transitions from magma-poor margins to oceanic crust have been described in the literature²⁴, as have transitions from magma rich margins to oceanic crust²⁵. Long-term generation of magma poor ocean floor by faulting and mantle exhumation^{26,27} at spreading centers has also been documented. It is evident that opening modes of continental margins depend on magma budget or onset time of volcanism²⁸. Flood basalts forming seaward dipping reflectors (SDRs) with associated deeper magmatic additions and intrusives²⁹ characterize magma-rich margins³⁰ often

¹Hess Corporation, 1501 McKinney Street, Houston, TX 77010, USA. ²Université de Strasbourg, CNRS, ITES_UMR, 7063 Strasbourg, France. ³Present address: Ormat Technologies, 6140 Plumas Street, Reno, NV 89519, USA. ✉e-mail: bkilsdonk@hess.com

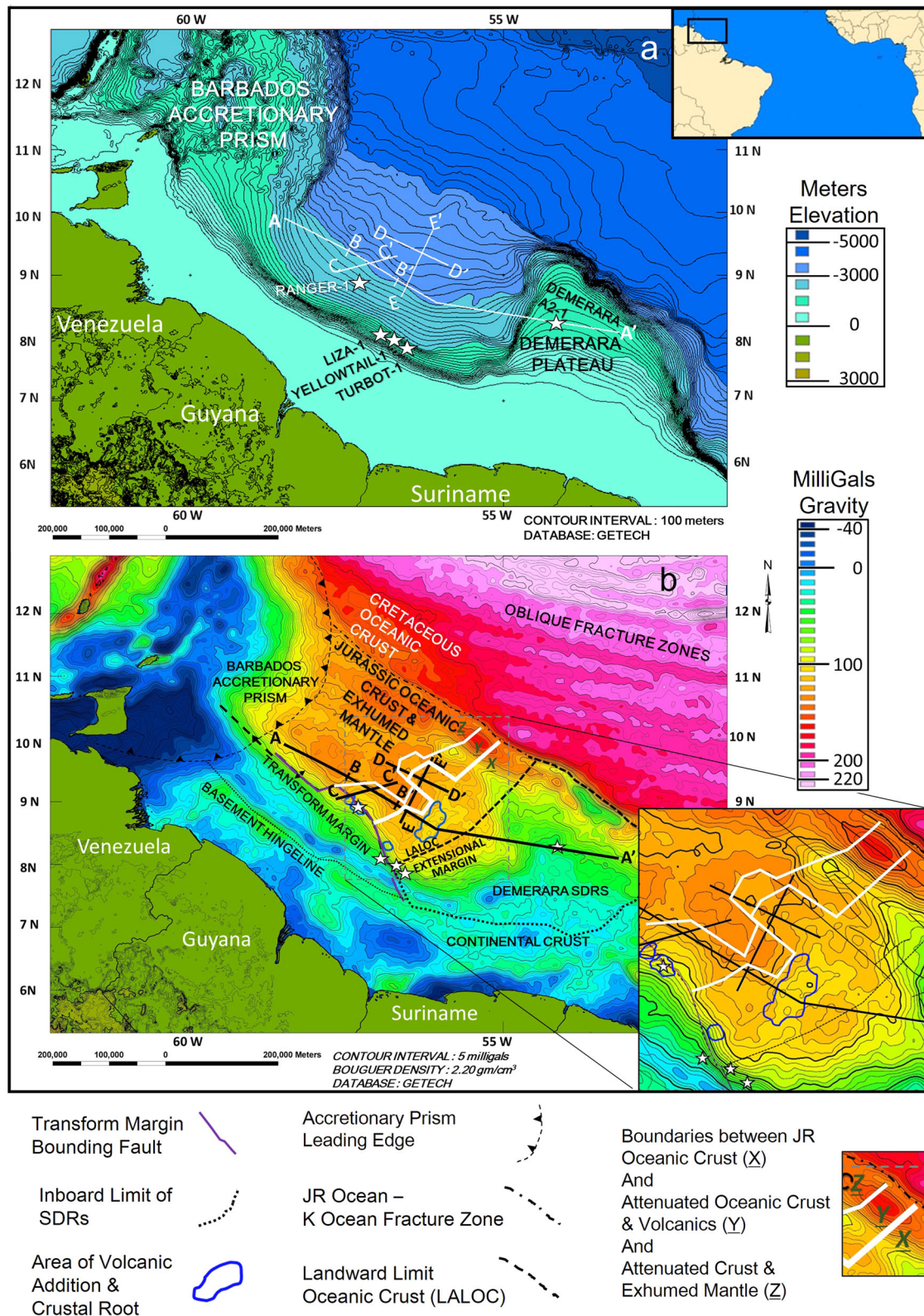


Fig. 1 | Bathymetry and gravity maps with data locations. **a** Location of seismic lines from Figs. 2–4 overlain on bathymetry/topography from a DEM (Digital Elevation Model) compiled by Getech Inc. Location of the wells Ranger-1, Liza-1, Yellowtail-1, Turbot-1, and Demerara A2-1 are shown. The primary bathymetric data source for this compilation is GEBCO 2020⁶⁵ which was combined with other marine surveys. The topography data is from SRTM15 + V2⁶⁶. **b** Bouguer gravity

anomaly map compiled by Getech Inc. A 3D Bouguer correction, with density 2.20 g/cm^3 , was applied to the Free Air anomaly. Simplified tectonic boundaries are based on all available geologic/geophysical data. LALOC Landward Limit of Oceanic Crust. Inset map in lower right to clarify link between seafloor Bouguer character and crustal structures in Figs. 2–4. Thin black lines in the NE part of the inset map show the structural grain from published fold axes and fault traces⁴.

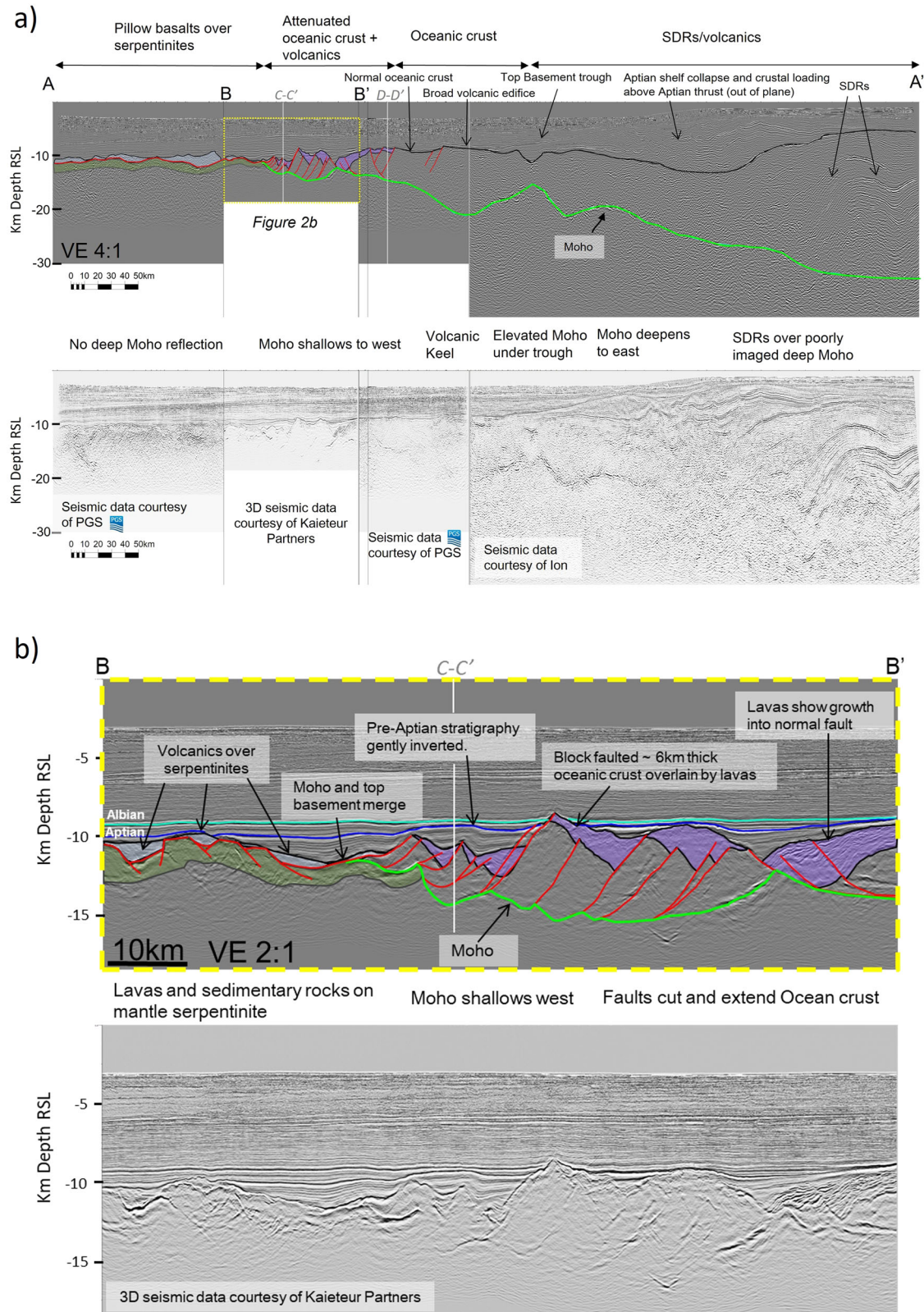


Fig. 2 | Interpreted and uninterpreted seismic transects A-A' and B-B'. Locations shown in Fig. 1. **a** Regional line A-A' trending from inboard (southeast) to outboard (northwest) in the direction of Jurassic extension. The Demerara plateau (southeastern end of line) is underlain by stacked flood basalts. These transition westwards to SDRs and eventually oceanic crust. The Moho reflection rises to the west. Note the elevated Moho and elongate trough feature at the transition from SDRs to oceanic crust. This relationship extends over 120 km along the trough. Farther northwest the normal oceanic crust is faulted into a series of fault blocks. **b** line B-B' inset from (a).

Normal faults detach on or into the Moho and bright, high impedance events, interpreted to be volcanic growth strata, fill graben. The Moho rises to the northwest under the fault blocks, reaching the base of the layered sedimentary pile. At the western end of B-B' the Moho reflection transitions to an undulating discontinuous surface, overlain by an irregular topped interval interpreted to be pillow basalts, and underlain by serpentinitized mantle. The apparent slight inversion is from Aptian shortening directed largely out of the plane of this transect¹. No deeper Moho event is visible in this area.

associated with mantle plumes and overlying hotspots. In such cases, SDRs commonly transition outboard to normal ocean crust³¹. In contrast, magma-poor margins are characterized by hyperextended continental crust often culminating outboard in exhumed mantle^{32–34}. Nevertheless, these characterizations and models of rift-to-drift evolution^{24,25,32} do not adequately account for observations of magmatic and tectonic transitions along the Guyana/Suriname Margin.

Multiple discoveries in Guyana, including the 2015 Liza field and related discoveries, found over 11 billion barrels of recoverable oil equivalent³⁵. Seismic acquisition and reprocessing following initial exploration success images deep structures and the deep crustal architecture. Desire to extend exploration success eastward drove complimentary long-offset seismic programs in Suriname with complimentary deep images of the eastern margin and Demerara Plateau⁴.

We present newly reprocessed seismic images from 2D and 3D datasets that show the deep structure, including the Moho, of the Guyana/Suriname margin offshore northeastern South America (Fig. 1). We also present integrated analyses of gravity and magnetic data and couple these with implications from plate models. These data provide a fuller understanding of the continuous tectonic and magmatic evolution of this margin, from the flood basalts of the Demerara Plateau to mantle exhumation on the deep-sea floor. Clearly imaged primary tectonic features – Moho, major faults, volcanics, and top basement – and their signatures on Bouguer gravity maps, constrain the spatial distribution of tectonic domains and their relative temporal evolution.

The data show a full and continuous evolution from a magma-rich continental margin, through 6–7 km thick, tabular oceanic crust, to late-stage seafloor spreading by faulting and mantle exhumation. Different magma budgets must have operated through different stages of margin evolution as proposed by Pindell et al. for the Gulf of Mexico^{36,37} and by Pindell and Heyn⁵ for both the Gulf of Mexico and the Central South Atlantic. The temporal and spatial tectonic organization of the Guyana/Suriname margin contrasts sharply with magma-poor margins that evolved from initial extension through mantle exhumation and culminated with the creation of normal, tabular, 6–7 km thick (Penrose type³⁸) oceanic crust³⁹, as well as with magma rich cases that evolved from large SDR packages to normal oceanic crust²⁵. The complete evolution, apparent on this margin, also contrasts with descriptions of magma-poor spreading centers that lack the context of development from a continental margin^{14,26,27}. Estimating volumes, timing and rates of magmatic additions remains difficult, but the Guyana/Suriname margin data we present offer a unique view of a complete transformation from an initially magma-rich margin with thick SDR geometries through normal steady state 6–7 km thick tabular oceanic crust commonly associated with fast spreading ridges^{21,38}, to magma-poor mantle exhumation of the type characteristic of slow spreading ridges^{14,21,26}.

Results

Demerara SDRs

Prominent bright reflections diverge and increase in dip westwards on the western margin of the Demerara Plateau (Fig. 2a). The reflections fade at depths that rise from 22 km in the east to 11 km in the west. Reuber, et al.⁶ interpret these events as volcanic seaward dipping reflectors (SDR). Subsequent interpretations of the same data agree¹ and dredge samples³ confirm Middle Jurassic magmatism on the northern edge of the Demerara Plateau.

Crustal trough

The top of oceanic crust is depressed in a 120 km long trough (Fig. 2a) just outboard (west) of the SDRs. This trough is 2 km deeper than the surrounding crust, 20–30 km wide, and located above a variably well imaged Moho high in an elongated zone of thin crust that trends northeast-southwest. The same depression is interpreted on seismic based transects of Museur et al.² and Graindorge et al.¹. A similar crustal thin on the Namibian margin was described first by McDermott et al.⁴⁰ and later by Geoffroy et al.⁴¹.

Normal and faulted oceanic crust

Much of the deep basin is floored by a roughly horizontal top basement seismic reflector 6 km to 6.5 km above a parallel Moho reflector (Fig. 3a, b) characteristic of normal, Penrose type, oceanic crust^{38,41}. This largely undeformed oceanic crust forms a domain outboard of both the crustal trough and Demerara SDRs. It transitions abruptly into an area of faulted and extended crustal blocks with high amplitude graben fill (Fig. 3a). The line of transition is stepped (Fig. 1b) and offset by fracture zones that influenced and segmented later deformation. A transect (Fig. 3b) across major fracture zones images areas of intact normal oceanic crust alternating with areas of oceanic crust extended at a high angle to the transect. The transition from constant thickness crust to extended and attenuated crust is apparent both on seismic images (Figs. 2–4) and on the gravity map (Fig. 1b).

A set of ~6 km thick crustal fault blocks with parallel top basement and Moho events are imaged in Fig. 2b between areas of more intensely thinned crust. Tilt angles of fault blocks increase to the northwest, and bounding fault dips decrease. Each block is buried by growth strata that expand towards bounding faults. High-impedance reflectivity within the expanded graben suggests volcanic fill.

Volcanic edifice

A local volcanic edifice surrounded by normal thickness oceanic crust forms a broad basement high west of the crustal trough on Fig. 2a. A Moho deep or “keel” that underpins and isostatically supports the high is apparent on seismic images and gravity maps (Fig. 1b). Although it is not the only volcano on the margin, this feature is anomalous within a broad surrounding area of normal thickness oceanic crust (Fig. 3a, b). That crust, although locally rotated by extensional block faults farther outboard, commonly exhibits a nearly horizontal top roughly 6 km above a parallel Moho. The 2018 Ranger-1 hydrocarbon discovery was made above a crustal high with bright reflectivity and bidirectional dip in its upper 5 km⁴. It is underlain by a three-dimensional keel, similar to that in Fig. 2a, suggesting similar volcanic origins.

Moho, top basement, and exhumed mantle

Depths and geometries of seismic reflections change markedly from east to west on Fig. 2a. The Moho at the eastern edge of the transect is not well imaged but must be below the deepest imaged SDRs – at least 30 km deep, in agreement with seismic refraction and velocity analyses^{2,42}. To the west, a clear Moho reflection rises from ~22 km to 11 km. In all, the Moho rises a minimum of 19 km over a 120 km span. It is continuous with the oceanic Moho at the base of ocean crust fault blocks (Fig. 2a, b). Above the rising Moho, the top of the basement deepens from 5 km over the SDRs to 11 km just west of the oceanic fault blocks where the top basement and Moho reflectors merge (Left center of Fig. 2b).

Northwest of the merged basement-Moho reflectors, the base of the layered sedimentary section is characterized by a bright, semi-discontinuous reflection that is variably underlain by 0–3 km of apparently heterogeneous material. Large areas below the bright event are seismically transparent, lacking deeper reflectivity, while other areas contain dipping reflectors within or adjacent to volcanic highs¹³. The event itself varies from smooth and undulating where it approaches or merges with the Moho event, to rugose where it overlies structures between it and the Moho. That outboard seismic character persists through the western Guyana/Suriname Margin from the fault blocks of oceanic crust to the Barbados prism.

Transform margin and thrust offset Moho

An east-northeast to west-southwest trending seismic transect, normal to the shear margin (Fig. 4) shows attenuated continental crust in fault zone contact with crust of roughly normal oceanic thickness. Farther northeast the Moho reflection rises towards the deepening top basement reflection, and both are offset by a thrust fault. Northeast of the thrust, the Moho and top basement events merge and display the seismic character that persists northwest to the Barbados accretionary prism. Crests and troughs of the

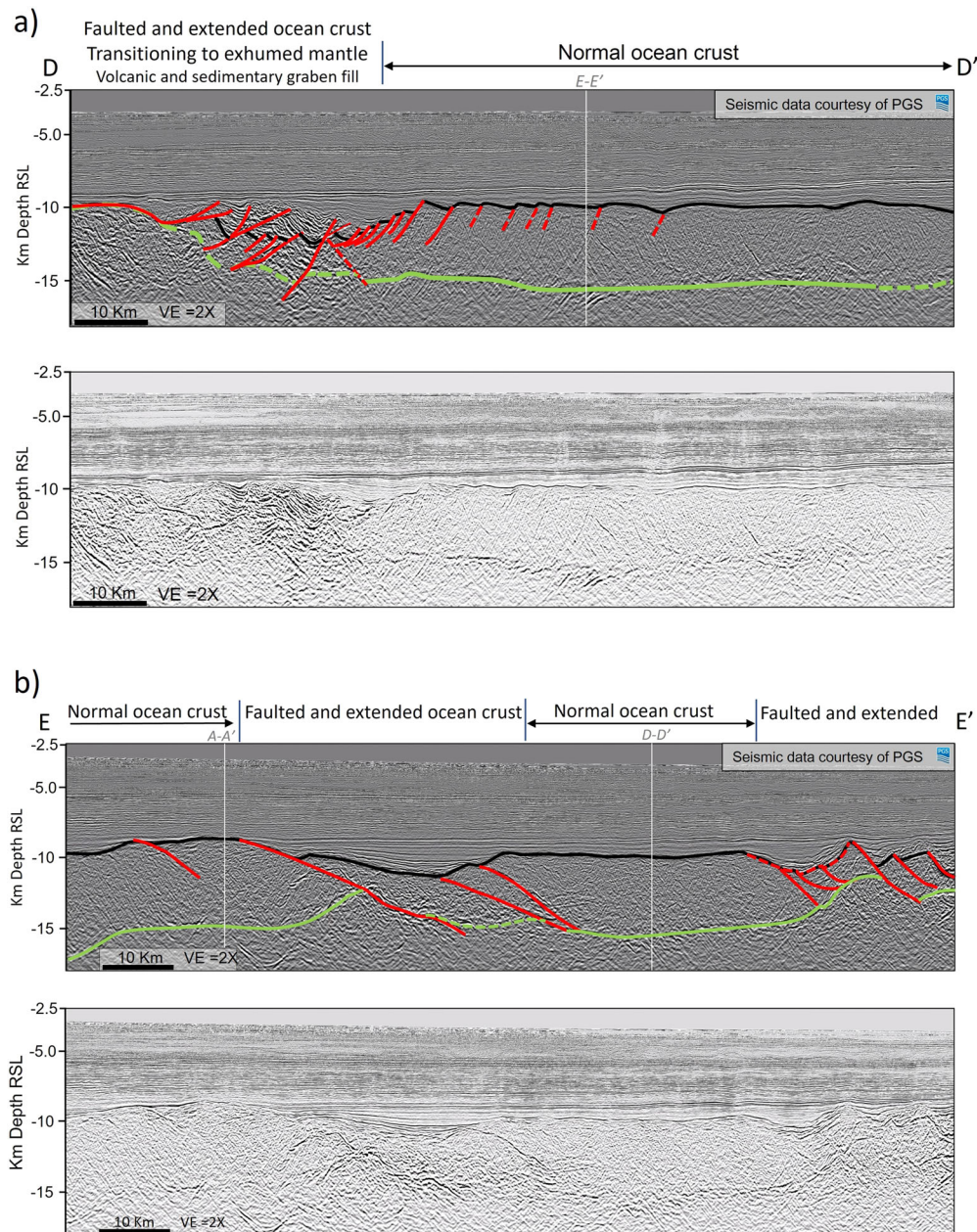


Fig. 3 | Interpreted and uninterpreted seismic transects D-D' and E-E'. Locations shown in Fig. 1. **a** Seismic transect D-D' is sub-parallel to the northwest-southeast direction of Jurassic plate separation. Parallel horizontal top basement and top Moho reflections define constant thickness oceanic crust in the southwestern part of the transect. Normal faults cut and extend the ocean crust to the northwest. High amplitude events in half-graben fill are interpreted to contain volcanic flows. The

structures are largely extensional on this transect but also affected by out-of-plane Aptian aged shortening. **b** Seismic transect E-E' at a high angle to the direction of Jurassic extension. Lateral transitions from constant thickness ocean crust to crust extended at a high angle to the plane of the section are interpreted as original fracture zones that were re-utilized during subsequent extension. Jurassic extensional structures are clear but have been modified by later Aptian shortening.

folded deep top basement and shallow Moho have relief on the order of 1000 m. Fold axes trends and the thrust's strike are roughly northwest-southeast (Fig. 1b) consistent with compressional structures throughout the margin⁴.

Integrated geophysical transect

A 2D transect (Fig. 5) correlates gravity and magnetic anomalies with structural/tectonic boundaries imaged by seismic data. It trends northwest to southeast across the Guyana/Suriname Margin. The magnetic signal over the Demerara Plateau shows a pattern of highs and lows more variable than depths to top SDRs. The sinusoidal character of the anomaly profile resembles those over well-defined oceanic crust⁴³. However, Geoffroy et al.⁴⁴

demonstrate that this type of anomaly character can occur over well imaged SDRs laid down on attenuated continental crust. The source of variability lies within the Demerara SDR sequence, from the top layer down to the Curie depth calculated as 22 kilometers from the regional magnetic database⁴⁵ (Supplementary Note 1 and Supplementary Fig. 1). Dredge samples and plate models^{1,3,5,6} imply SDR emplacement from Pliensbachian (186 Ma) to Callovian (166 Ma) during numerous and rapid magnetic polarity reversals⁴⁶⁻⁵⁰. Basalt flows have a broad range of magnetic susceptibilities and, in general, a Königsberg ratio > 1 (the ratio of remanent magnetization to induced magnetization)⁵¹. Therefore, observed anomalies arise primarily from juxtaposition of flows having different ages and magnetic polarities, however variations in magnetic susceptibility also contribute anomalies to

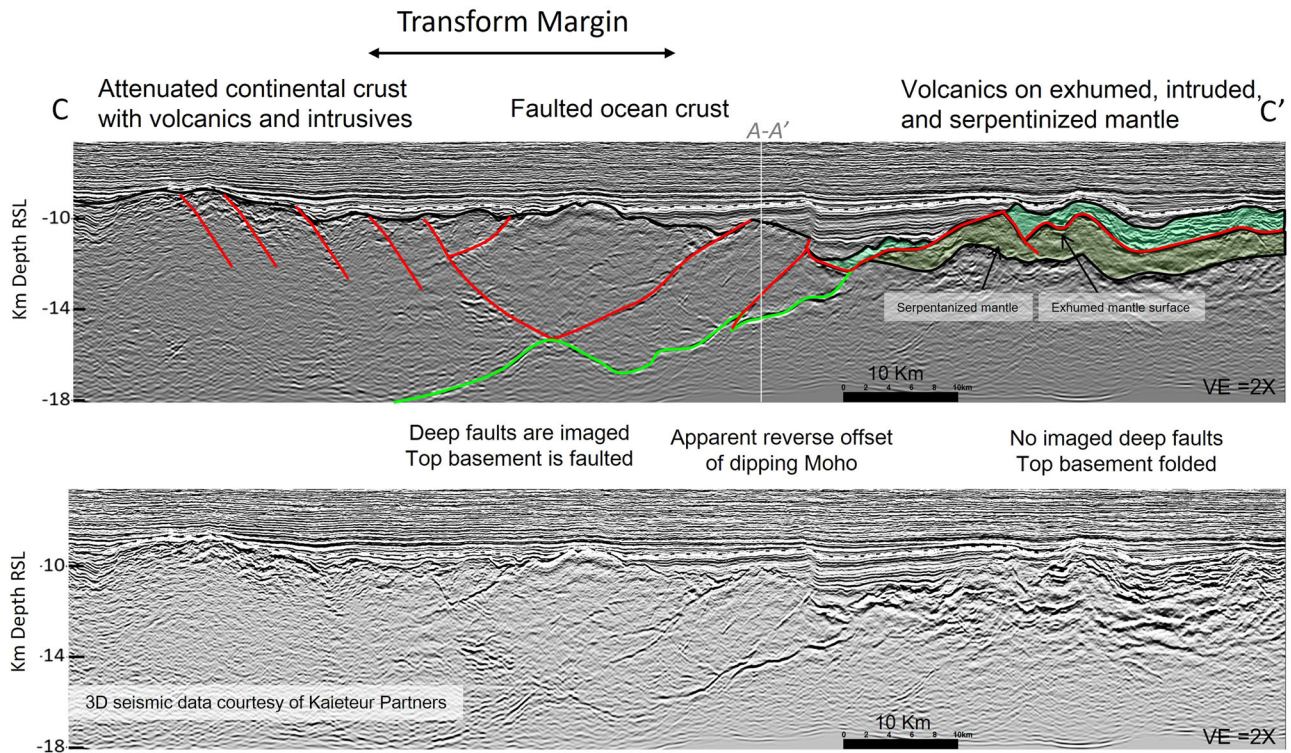


Fig. 4 | Interpreted and uninterpreted seismic transect C-C'. Locations shown in Fig. 1. Seismic transect at a high angle to Jurassic extension but roughly parallel to Aptian shortening. The transition from thick crust and deep Moho in the southwest to exhumed mantle in the northeast occurs over tens of kilometers. Northeast of the thrust, the point where the Moho reflection disappears below the layered sediment pile approximates the southwestern edge of exhumed mantle. Northeast of that

point, the top mantle surface is bright, shallow, folded, and directly overlain by submarine extrusives and layered sedimentary rocks. Southwest of that line, the Moho is well imaged, shallowing to the northeast, and clearly offset by a thrust that was active during Aptian northeast-southwest shortening. Dashed white line is the top of Aptian stratigraphy.

the observed signal. Rapid Middle Jurassic polarity reversals combine with Aptian folding of the SDRs for a complex magnetic signal. The anomalies on the profile are difficult to correlate in a regional perspective given that our magnetic maps over the Demerara Plateau are gridded from multiple surveys with highly variable line spacing and azimuths. This also results in difficulty in comparing the Demerara magnetic maps with surveys designed to provide ideal measurements of SDR geophysical signals⁴⁴. On the cross section, the number of observed magnetic anomalies correlated to Demerara SDRs is fewer than the number of time equivalent polarity reversals^{46,47} for at least two reasons. 1) Episodic emplacement diminished the number of recorded reversals because flows during some periods were thin or absent and thus contributed little or nothing to the anomalous magnetic field. 2) Magnetic variations in overlying SDRs may partly or totally mask magnetic contrasts of deeper units.

Free air gravity anomalies correlate with density contrasts from the seafloor to the mantle. Because the highest density contrast occurs at the seafloor, bathymetric variations dominate the signal. The Bouguer correction removes, or at least dampens, bathymetry-induced anomalies. Profiles of both the free air and Bouguer-corrected gravity above the 2D model facilitate correlation with the geologic density structure (Fig. 5). At the edge of the Demerara Plateau, water depths increase to the northwest from 1200 m to 3000 m and, as a result, the free air gravity along the profile drops by 35 milligals. In contrast the Bouguer gravity over the same span decreases in the opposite direction to the southeast, signaling southeastern deepening of Moho beneath the plateau.

The southeastern drop in regional Bouguer anomaly (Fig. 5) along most of the transect correlates to a dramatic deepening of the Moho. However, a local decrease in Bouguer gravity at the far northwest of the transect is an out of plane signal from deeper Moho below continental crust juxtaposed across the transform margin, as the line of section edges nearer that boundary (Fig. 1b). Accounting for this local out of plane affect, the

gravity data are consistent with an observed Moho reflector that shallows to meet the base of apparent layered stratigraphy (Fig. 2a) in the northwestern quarter of the transect. Sedimentary rocks sit directly upon exhumed, serpentinized mantle. Normal ocean crust is absent.

We model downward decreasing fractions of serpentinite in the serpentinization front⁵² as discrete layers with downward increasing density. The average thickness of serpentinized mantle is less than 4 kilometers. The region of mantle exhumation transitions eastward into a heterogeneous zone that mixes serpentinized mantle with blocks of extended, faulted and disjunct oceanic crust. We model oceanic crust with two density layers based on published reports of cores and cuttings^{53,54}. Both the Bouguer and free air anomalies have low amplitude southeast dipping gradients through the serpentinized zone. Because densities of serpentinized mantle and ocean crust are similar, the gradient must come from the eastward increase in mantle depth. The heterogeneous zone transitions eastward to a broad volcanic edifice and underlying keel where magmatic additions locally thickened the previously 6 km ocean crust to more than 12 km. The resulting Moho depression produces a 17 milligal gravity minimum.

The LALOC (Fig. 1b) lacks a distinctive gravity anomaly because there is no impacting density or thickness contrast between inboard SDRs and outboard oceanic crust. Farther southeast, Jurassic magmatic additions floor much of the Demerara Plateau. Massive outpourings of high-density (2.80-2.92 gm/cc) basalt flows, with associated feeder dikes and deep magmatic additions, thickened the crust to load and flex the mantle to below 30 km and create a deep crustal root that isostatically balances the shallow bathymetry of the Plateau. A Bouguer gravity minima correlates directly with the seismic image and interpretation of the deep Moho.

Plate model

There is general agreement that the Demerara and Guinea Plateaus formed during the middle Jurassic over a hotspot that moved away after building the

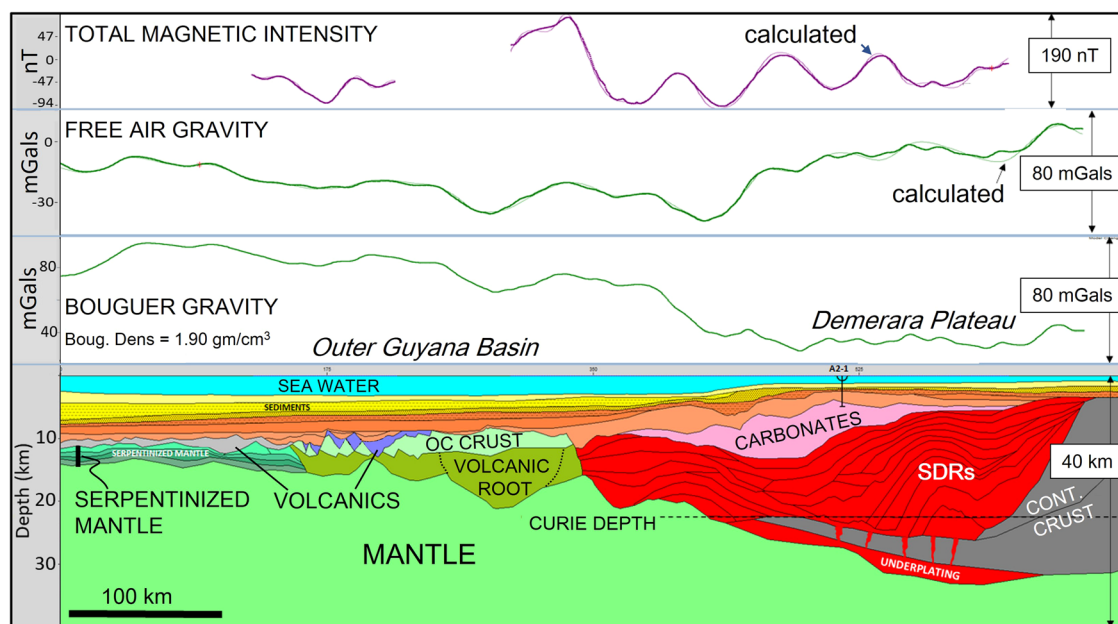


Fig. 5 | Regional geophysical model of the outer Guyana Basin and Demerara Plateau along the seismic line in Fig. 2a. The model is based on all geologic and geophysical data and current regional tectonic concepts. The change in crustal thickness and lithology interpreted along this model profile reflects the dramatic variation in magma budget in space and time in the region. The correlation between the observed (thick) and calculated (thin) Free Air gravity anomalies, as well as the regional trend of the Bouguer gravity anomaly field, supports the seismic

interpretation of a regional downward flexure, increasing to the east, of the dense underlying mantle responding isostatically to magmatic addition. The sinusoidal nature of the observed Total Magnetic Intensity anomaly is the response of complex magnetization in the Demerara Plateau SDR packages beneath their gently dipping top surface. Geophysical construction is described in Supplementary Note 2 and detailed parameters are given in Supplementary Fig. 2 and Supplementary Table 1. Data based determination of the Curie depth is shown in Supplementary Fig. 1.

plateaus. There is some disagreement, however, over the subsequent path of the hotspot. At least two have been proposed. Reuber et al.⁶, Pindell and Heyn⁵, and Pindell, et al.³⁶ track the hotspot onto the conjugate North American Plate in the Late Jurassic to build the Bahamas Bank volcanics continuously until ceasing in the Aptian. Basile et al.³ reconstruct the Sierra Leone hotspot track back to the Demerara and Guinea Plateaus and account for an 80 Ma gap in surface volcanics, from 170 Ma to 90 Ma, by unfavorable tectonic position. We adopt the hotspot track of Pindell and Heyn⁵ in our plate reconstructions but stress that our observations of the Guyana Margin evolution imply the cessation of SDR flood basalts prior to accretion of normal oceanic crust. They do not depend on the path the hotspot might have taken after construction of Demerara and Guineas Plateau SDRs.

During the Early to Middle Jurassic (Fig. 6a), the continental crust extended as Pangea began to break apart⁵⁵. Large volumes of extruded magma formed the Demerara and Guinea Plateaus³ and, by inference, the Bahamas Bank on their central Atlantic conjugate. The magmatic outpouring occurred episodically over a period of approximately 20 million years based on the extent of the SDR domain and the Central Atlantic opening rate⁴⁸ in our plate model. Dredge samples from the northeastern flank of the Demerara Plateau recovered volcanics of Aalenian age³ (173.4 Ma). Volcanism diminished as plume influence waned at least partly, and perhaps wholly, as the margin moved away from the hotspot at the plume head. By 160 Ma the mantle plume was located beneath the crust of the North American plate^{5,6} (Fig. 6) and the related hotspot began building the long volcanic promontory of the Bahamas Bank. Plume-related magmatism largely ceased on the Demerara and Guinea Plateaus and normal (6–7 km) thickness oceanic crust began to form in the Callovian. The spreading center northwest of the developing margin was in place by the Oxfordian (Fig. 6b).

For the next 40 million years the Guyana/Suriname Margin expanded and subsided at a plate intersection connecting the Central Atlantic to the Proto Caribbean (Fig. 6b, c). The South American and northwest African Plates moved southeast as a unit relative to the North American Plate. In the Aptian the African Plate began to separate from the South American Plate

(Fig. 6d)⁵⁶. This motion was initially transpressive in the Guyana/Suriname margin, evidenced by NE-SW shortening of the Jurassic oceanic crust of the outer Guyana/Suriname Margin and the crust flooring the Demerara Plateau. After initial compression, the equatorial Atlantic opened by seafloor spreading in a direction locally oblique to the northeastern boundary of the Guyana/Suriname margin.

Discussion

Changes in Moho depth in the northwest-southeast direction of plate separation mirror changes in paleo-seafloor composition and deformation. The Moho is deepest, at least 30 km (Fig. 2a) below the deep diffuse truncations of the imaged Demerara SDRs, and in broad agreement with results from refraction data^{3,42}. The Moho rises to the northwest beneath what's been interpreted as SDRs overlying extended lower continental crust¹ or alternatively in our model (in Fig. 5) by a similar combination in the east yielding to a fully magmatic crust in the west. We adopt an end member model of a fully magmatic crust for two reasons. 1) Removal of the magmatic portion in plate reconstructions collapses the Jurassic predecessor of the Demerara Plateau and produces a tight fit to North America without invoking major, but unseen, continental shear zones. 2) Magnetic data from the Plateau to the oceanic crust require polarity reversals in units down to the Moho (or curie depth where shallower) to match the observed magnetic signal. However, the data cannot differentiate between deep SDRs, an associated feeder system, or contemporaneous intrusions as the source of the deep reversals. The Moho spikes upward below a crustal trough at the boundary between the Demerara Plateau and oceanic crust. Outboard of the trough the crust is largely of normal thickness with top crust parallel to oceanic Moho. It is, however, locally thickened by volcanoes and their associated roots. Farther west the oceanic Moho is broken and rises across faults until it merges with the top basement.

Westward shallowing of the Moho (Figs. 2, 3, 5) coincides with westward increases in extension, crustal thinning – ultimately to the point of mantle exhumation – and local submarine volcanics that were apparently contemporaneous with extension. The outboard mantle is exhumed where

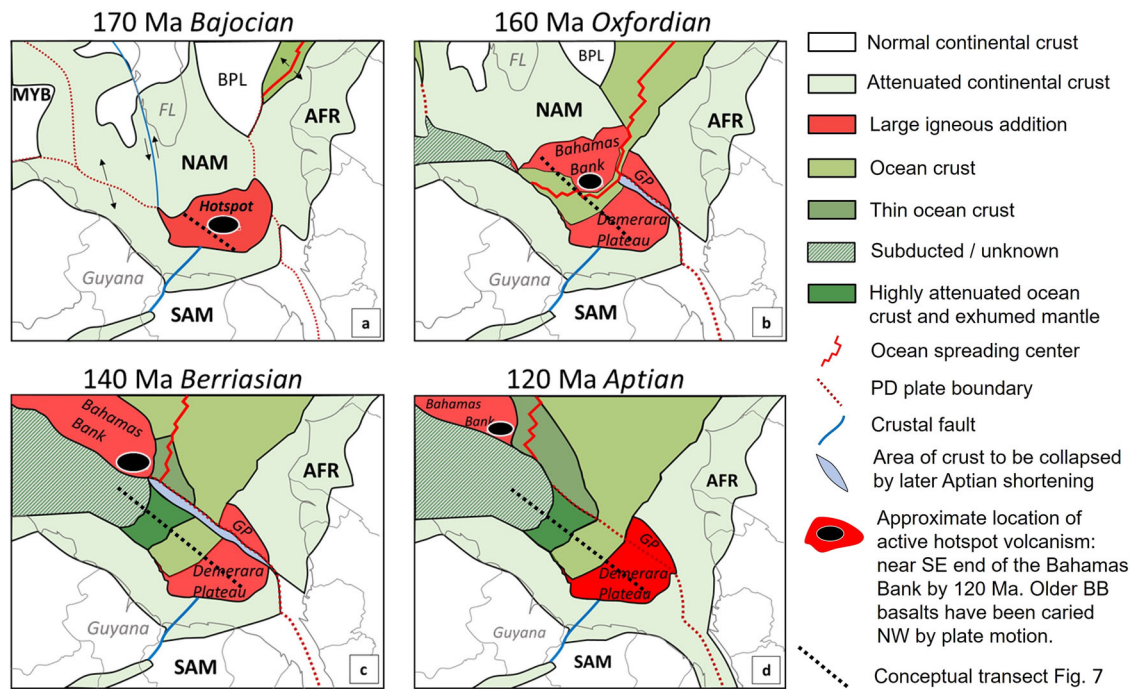


Fig. 6 | Plate reconstructions. These time sequences are interpreted from all available geologic and geophysical data, using PaleoGIS (The Rothwell Group) software. The initial model⁴⁸, developed at the University of Texas, Austin, provided the starting point and basis for our model. Modifications incorporate elements of crustal stretching and variations in crustal boundaries as well as minor changes in poles of rotation. Notional location of conceptual transect (Fig. 5) shown as dashed line. **a** 170 Ma - Bajocian; seafloor spreading begins to encroach from the north; crustal attenuation and rift related volcanism along the Guyana transform margin; expulsion of magmas (SDRs) on the Demerara Plateau, Bahamas Bank (BB), and the Guinea Plateau (GP). BPL is the Blake Plateau and MYB is the Mayan Block. **b** 160 Ma - Oxfordian; oceanic crust developed along the Guyana transform margin

and the northwest boundary of the Demerara Plateau; continuation of expulsion of magma on Bahamas Bank; expulsion of magma has ceased on Demerara Plateau and Guinea Plateau. Note the zone of crustal shortening between the South American and African plates. **c** 140 Ma - Berriasian; passive margin subsidence and continued formation of oceanic crust and exhumed mantle flooring the outer Guyana Basin and the adjacent African margin. The active Bahama banks hotspot is now in a distal position to the basin. **d** 120 - Aptian; crustal shortening in the oceanic domain and between the volcanic additions of the Demerara Plateau and Guinea Plateau. The Equatorial Atlantic begins to open.

mantle and top crust reflections merge. By analogy with documented cases^{57–59} we interpret the top mantle as a serpentinized⁵⁸ mantle-exhumation fault, that replaced magmatic generation of oceanic crust at a ridge as the mechanism of plate separation. The exhumation fault is now covered with a variable-thickness carapace with a distinct, commonly non-layered seismic character consistent with mounded sporadic igneous extrusive rocks. Eruptions must have been subaqueous to deposit lava directly on the exhumed mantle. Therefore, we interpret the carapace as pillow basalts. That carapace is itself overlapped and overlain by a layered sequence of sedimentary rocks.

The undulating, folded morphology of the shallow outboard Moho contrasts with the block faulted oceanic crust to the east (Fig. 2a, b). It was folded during the Aptian shortening that is recorded by parallel folds nearer the plate boundary to the northeast^{4,60} and by the crustal thrust in Fig. 4. We suspect that the crustal thrust (Fig. 4) may have originated as an oceanic fracture zone oriented favorably for reuse during the Aptian shortening event.

We see two possible origins for the elongate trough separating the Demerara Plateau from normal thickness oceanic crust (Figs. 2b, 7b). (1) It formed as an extensional neck in the oceanic crust, localized at the edge of the Demerara Plateau. In this case the trough would be contemporaneous with the first normal faults to extend the ocean crust. (2) It formed as originally thin crust, responding to a temporary magma deficit after hotspot generated SDR formation but before decompression driven generation of normal thickness oceanic crust. Although these processes may have both contributed, we favor the second for three reasons. (1) It is consistent with the sequence of crustal accretion and deformation progressing from inboard to outboard indicated by our data and common on other margins^{32,34,39}. (2) It

is consistent with slow, normally magma poor²¹, spreading rates from our plate model during, and just after, hotspot departure. (3) Trough fill appears non volcanic with unrotated horizontal layering and lacks large faults. It is unlikely to be the same age as high amplitude, rotated, faulted fill in outboard grabens.

Geoffroy et al.⁴¹ propose a different origin for a crustal thin offshore Namibia. They interpret crust thicker than standard oceanic, but outboard of SDRs, as lower continental. In their model the crustal thin is localized at a breakaway fault that decouples the upper crust and SDRs from lower continental crust in the crustal thick. Although we cannot rule it out, we do not apply their model to the Guyana/Suriname margin largely because the structures of the two margins are different. The anomalous crustal thick on the Namibian margin is elongated and persists outboard of the crustal thin. It does appear as if the two are related. In contrast, there is well-imaged 6–7 km thick oceanic crust just outboard of the crustal trough on much of the Guyana/Suriname margin, the region of thick crust is less elongated, and its long axis does not parallel the trough. We interpret the thick crust as a local, but large, volcanic edifice that postdates the formation of the oceanic crust. The initially 6–7 km thick crust has been locally thickened by magmatic addition, potentially contemporaneous with the formation of the Ranger volcanic high and underlying root⁴ and the apparently volcanic graben fill to the northwest.

Regional well correlations date the stratigraphy over rift structures (Fig. 2b) as pre-Aptian but no more precisely. However, volcanic graben fill expands into bounding faults and is clearly syn-tectonic. Those volcanics are likely to be the same, or similar age as volcanics on the exhumed Moho. That age relationship implies that mantle exhumation post-dated formation of normal-thickness ocean crust. Exhumation was the final stage in the

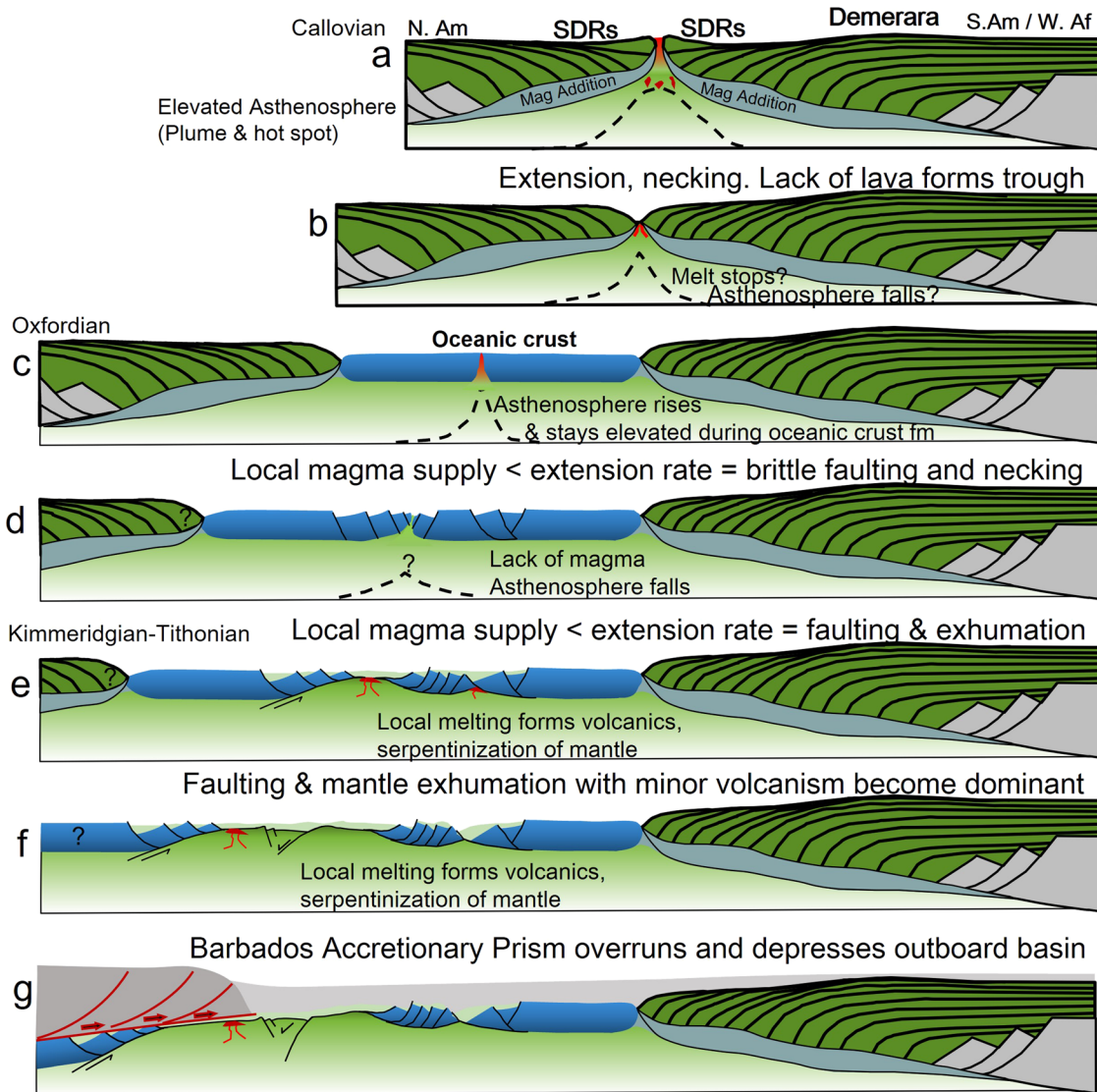


Fig. 7 | Conceptual formation of the Guyana Basin, notional location in Fig. 6. a SDR formation when magma supply > extension rate. b Magma supply < extension rate leads to thin crust and mantle stretching. This causes the asthenosphere to rise. c Rising asthenosphere causes adiabatic melting and further production of magma leading to formation of normal oceanic crust (extension = magma supply). d Relative drop in magma budget (magma supply < extension rate) causes extension to be

accommodated in brittle extensional faulting of oceanic crust. e Brittle extension continues until the Moho is close to the sea floor and oceanic mantle is serpentinized (magma supply « extension). Limited volcanics fill grabens and cover exhumed mantle. f Extension by mantle exhumation continues as the dominant form of crustal formation. g The Barbados accretionary prism obliquely overthrusts extensional complex from plate separation at the western end of the drawing.

transition from magma rich to magma poor basement formation that progressed both through time and from east to west through the margin.

An extensive sequence of SDRs in the 30 km thick, rooted Demerara Plateau at the eastern edge of the basin point to sub-areal plume-driven hotspot volcanism that overwhelmed early continental separation. Westward those SDRs transition to younger, normal thickness, oceanic crust (Fig. 2) across an elongated crustal trough that marks the transition from plume-derived magma to decompression-derived magma. Constant thickness ocean crust, locally thickened by younger volcanoes, across the trough from the SDRs, indicates a temporary balance between separation and magmatic addition from decompression melting. Faulting and extension of the constant thickness crust indicate that the balance eventually waned, and extension outpaced magmatic addition. Extension on faults increases from east to west and ultimately exhumes mantle in the central Guyana Basin.

Magma-rich margins are commonly characterized by a progression from rifted continental crust, through transitional volcanic SDR sequences before developing distal normal thickness ocean crust^{61,62}. Magma-poor and

intermediate margins have been described as progressing from proximal magma-poor domains through hyperextended or exhumed domains to distal normal-thickness oceanic crust^{24,32}. In contrast, Guyana/Suriname margin data show relative magmatic budget generally decreasing through time, from mantle plume to mantle exhumation with intervening periods that generated a normal thickness oceanic crust and then extended that crust by faulting. Similarly, the Sao Paulo magmatic plateau off Brazil^{36,63} once spanned the conjugate margins of the central South Atlantic, like those of Demerara-Bahamas, but plateau-breakup was magma-poor or locally magma-moderate before more “normal” seafloor spreading began⁵.

We conceptualize a progression from mantle plume-generated SDR-dominated volcanic crust to lithospheric separation and generation of oceanic crust (Fig. 7a–c) through brittle extension and segmentation of the antecedent steady state crust (Fig. 7d, e) - contemporaneous with ancillary volcanics - to a penultimate state dominated by extensional exhumation of mantle with minor volcanics (Fig. 7e, f). Lastly, sediments have buried the margin as the Barbados accretionary prism obliquely overran its present-day northwestern boundary (Fig. 7g).

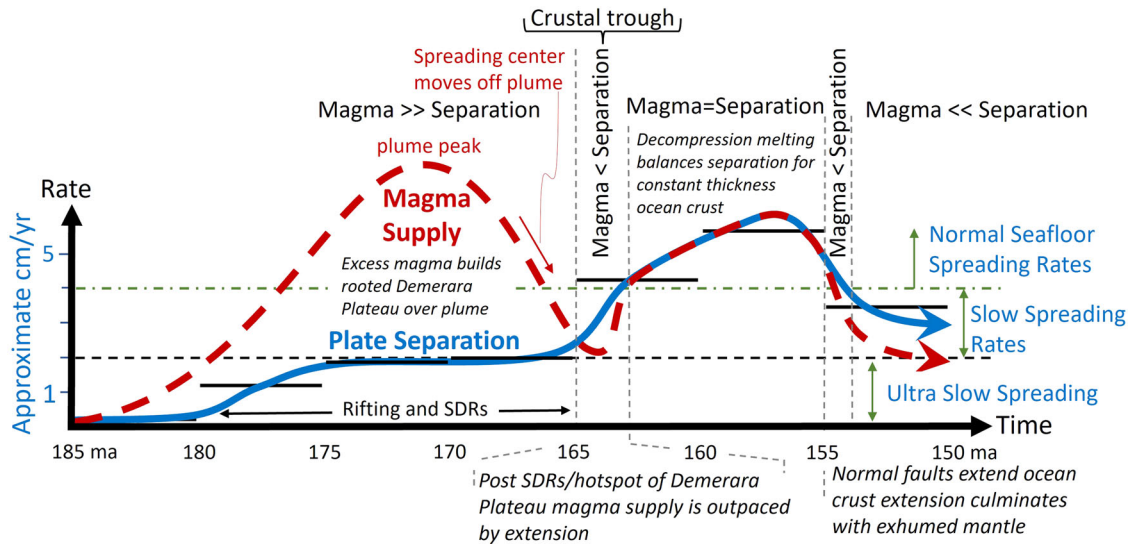


Fig. 8 | Rate competition between magmatic addition and mechanical extension during plate separation. Ages and rates are approximate but are based on constraints from our plate model (selected time steps shown in Fig. 6). Horizontal black bars show average rates approximated over 5 my intervals. The dashed blue curve labeled “Plate Separation” is a hand-drawn estimate of the continuously changing rate through time. The dashed red line shows relative excess, equivalent, or deficit magma relative to separation based on seismic observations in the text. The Demerara plateau was built during a stage when the volume of magma introduced greatly exceeded the room created by extension or separation (Magma » Separation). Tabular constant 6–7 km thick oceanic crust formed during a stage when the volume of magma balanced the room created by plate separation (Magma = Separation). Thin crust was created, and mechanical extension occurred, during stages when the volume of magma was insufficient to balance the room created by plate separation (Magma < Separation). The dashed green line at 4 cm/yr. separates slow spreading

rates, shown to be magma poor²¹, from normal rates that produce constant thickness oceanic crust. (I) Rifting rates were slow during the incipient stages of this margin, and plume-driven magmatism overwhelmed extension to build stacked SDR piles on the initially adjacent Demerara and Guinea Plateaus. (II) Magmatic activity slowed as the focus of extension migrated away from the mantle plume hotspot, which ended up on the NA plate in our model. (III) After the separation from the hotspot, the spreading rate increased, but was still slow (<4 cm/yr) and magma poor. (IV) Spreading rate increased to normal and generated constant thickness oceanic crust by steady state decompression melting. (V) The spreading rate dropped below 4 cm/yr. and decompression melts no longer balanced separation. Extension replaced magmatic addition as the mechanism of plate separation, initially leading to faulting of oceanic crust and later to mantle exhumation at what was presumably a slow-spreading ridge.

After excess magma built the volcanic plateau, and after the temporary imbalance implied by our interpretation of the crustal trough, the rate of decompression melting increased to keep pace with separation and build constant thickness oceanic crust (Fig. 7c). Seismic images of ocean crust establish that both normal seafloor spreading, and lithospheric separation occurred before mantle exhumation (Figs. 2, 3). Faulting of oceanic crust with volcanic graben fill suggests waning magma production relative to plate separation. Plate models indicate that, after plume related magmatism ceased, magma poor extension occurred during slow spreading. Extensional faulting of the Guyana/Suriname oceanic crust, transitioning to late-stage mantle exhumation on the seafloor, shows that normal oceanic crust is not necessarily the final stage of continental separation. Rather, as elsewhere on mid-ocean ridges²¹ the mechanism accommodating separation, either mechanical extension or crustal addition, depends on a rate competition between magma generation and plate separation⁶⁴ as illustrated in Fig. 8.

The observations here document a progression from (1) mantle plume and hotspot dominated magma rich continental break-up, through (2) thin post-hotspot crust, and (3) normal thickness oceanic crust that suffered late fault-dominated crustal extension, to (4) detachment-dominated formation of new sea floor and mantle exhumation. Alternate progressions on other margins might follow alternate variations in rates of magma generation and separation, but all margins should be described in terms of their entire structural/magmatic architecture in space and evolution through time^{5,20}. Competition between the rate of magma generation and plate separation determines which process, mechanical extension, or magmatic accretion, dominates at a specific time or location. The terms magma rich and magma poor are alone insufficient to describe margin evolution, and the generation of normal oceanic crust by decompression melting is not necessarily the end stage for an initially volcanic margin.

Methods

Seismic

Our results and conclusions are based on seismic images and interpretation of primary features - including top basement, Moho, faults, volcanoes, and igneous packages - coupled with gravity and magnetic analyses, plate models, and tectonic understanding drawn from cited literature. The organization and spatial relationships of these elements constrain the structure, evolution, and primary composition of the crust in the Guyana/Suriname margin. The seismic images here are extracted as a subset from larger data sets, but the data presented capture spatial and temporal transitions in crustal type and, coupled with plate reconstructions and with gravity and magnetic data, are sufficient to reproduce our main findings. The 2D seismic data in Guyana were acquired and processed as a multi-client survey by PGS in 2008 with 12 km streamer length and record length of 14 seconds. These Guyana data were reprocessed by PGS as a PSDM migration in 2017 on a proprietary basis. 2D seismic data in Suriname were acquired and processed by ION in 2012 with 10 km streamer length and 18 second record length. These Suriname data were reprocessed by ION in 2016 as a PSDM migration. The 3D data in Guyana were acquired by Polarcus for Esso Exploration and Production Guyana Ltd. and processed by CGG on a proprietary basis. We used plate reconstructions to give tectonic context for our seismic observations, constraining relative plate positions and tectonic rates.

Plate model

Our plate reconstructions incorporate all available geologic and geophysical data and are built using PaleoGIS (The Rothwell Group) software. Our full plate model is proprietary, incorporating elements of crustal stretching and variations in crustal boundaries, as well as minor changes in poles of rotation, but it is based on the Plates 2020⁴⁸ model developed by the University of

Texas at Austin, and produces reconstructions similar to multiple published examples^{5,6,56} for the area.

Bathymetry and gravity

Our bathymetry/ topography map (Fig. 1a) derives from a DEM (Digital Elevation Model) compiled by Getech Inc. using data primarily sourced from GEBCO 2020⁶⁵ but combined with data from other marine surveys. The topography data is from SRTM15 + V2⁶⁶. The Bouguer gravity anomaly map (Fig. 1b) was compiled by Getech Inc. It was derived from the Free Air gravity measured by marine gravity surveys and from satellite-measured variations in sea surface height. Application of a 3D Bouguer correction (density 2.20 g/cm³) dampened the signal associated with the large density contrast at the water bottom. The Free Air and Bouguer profiles that provide geophysical integration with our seismic-based 2D geophysical model were extracted from gridded maps. Short wavelength gravity anomalies arise from shallow density contrasts. Long wavelength anomalies arise from deeper contrasts, such as those produced by variations in Moho depth. Variations in Moho depth and crustal thickness derived from gravity anomalies agree with our seismic interpretations and define the 3D crustal architecture.

Magnetics

Total Magnetic Intensity data used to constrain and interpret our transect were acquired by two different marine surveys. The southeastern half of the cross section shows data acquired directly along the seismic line by ION GXT in 2013 during their 2D Guyana Span seismic acquisition program. The northwestern half of the transect shows marine magnetics acquired in 2018 as part of a 3D seismic acquisition program. We extracted that portion of the magnetic profile from a grid. We tied the magnetic anomalies of the two spatially separated marine surveys using an unpublished proprietary aeromagnetic survey that overlaps both. The induced magnetic field parameters for the study area are magnitude: 31,000 nanoTeslas, inclination: 22 degrees North, and declination 17 degrees West. In addition to the present-day inducing field, the paleomagnetic field has a profound effect on the magnetic signature of oceanic crust, SDRs and magmatic additions in general. To account for remanent magnetization in the model, we calculated the paleo-inclination and paleo-declination of cooling Demerara SDRs (at about 175 Ma) based on 1) reconstructions from the PLATES relative plate motion framework⁴⁸, and 2) the polar wander paths of Schettino & Scotese⁶⁷. The resulting paleo-inclinations and paleo-declinations were 14.75 N, 6.44 E. for normal polarity, and 14.75 S, 186.44 E for reverse polarity. In addition, we calculated the paleo-inclinations and paleo-declinations for oceanic accretion at 165 Ma as 10.0 N, 0.0E for normal polarity and 10 S. 180 E for reverse polarity.

Data availability

The bathymetry, topography, free air gravity, and Bouguer gravity data are available to license from Getech, Houston, Texas. The 2D marine gravity & magnetic data that support the findings of the 2D modeling are available to license from ION Geoscience, Houston, Texas. Restrictions apply to the availability of these data, which were used under license for the current study. The 2D seismic data in this paper are proprietary to PGS, ION, and GGMC – Government of Guyana. The 3D data were acquired by Polarcus for Esso Exploration and Production Guyana Ltd. and processed by CGG. They are proprietary to the Guyana Kaieteur block partners: Esso Exploration and Production Guyana Ltd., Ratio Guyana Ltd., Cataleya Energy Ltd., and Hess Guyana Exploration Ltd. Multi-Sat data are licensed through Getech Group plc, Kitson House, Elmete Hall, Elmete Lane, Leeds LS8 2LJ, UK, and shown with their permission. Seismic transects are published with permission from data owners and are extracted from larger data sets. Transects in Fig. 2b and Fig. 4 are not publicly available, they were extracted from a 3D volume proprietary to the Guyana Kaieteur block partners: Esso Exploration and Production Guyana Ltd., Ratio Guyana Ltd., Cataleya Energy Ltd., and Hess Guyana Exploration Ltd. Transects extracted from 2D data sets are owned by PGS ION, and CGG. PGS data,

acquired in a 2008 multi-client survey, were reprocessed on a proprietary basis by PGS in 2017. Restrictions apply to the availability of these data, which were used under license for the current study. Underlying 2D data may be available to license from the data owners.

Code availability

The Plate model software used for this study is available to license as PaleoGIS from the Rothwell Group, Lakewood, Colorado. Restrictions apply to the availability of this software, which were used under license for the current study, and are not publicly available. The gravity and magnetic modeling software used for this study are available to license as Oasis Montaj from Seequent Inc., Vancouver, Canada. Restrictions apply to the availability of this software, which were used under license for the current study, and are not publicly available. Generation of the magnetic power spectrum from total magnetic intensity and subsequent calculation of the Curie depth (Supplementary Note 1 and Supplementary Fig. 1) used Xcalibur Multiphysics software, which is available to license from Xcalibur Multiphysics, 10300 Town Park Drive, Houston, Texas 77072.

Received: 28 April 2023; Accepted: 12 February 2024;

Published online: 04 March 2024

References

1. Graindorge, D. et al. Deep structure of the Demerara Plateau and its two-fold tectonic evolution: from a volcanic margin to a transform marginal plateau, insights from the Conjugate Guinea Plateau. *Geol. Soc. Lond. Spec. Publ.* **524**, 339–366 (2023).
2. Museur, T. et al. Deep structure of the Demerara Plateau: From a volcanic margin to a Transform Marginal Plateau. *Tectonophysics* **803**, 228645 (2021).
3. Basile, C. et al. The Jurassic magmatism of the Demerara Plateau (offshore French Guiana) as a remnant of the Sierra Leone hotspot during the Atlantic rifting. *Sci. Rep.* **10**, 7486 (2020).
4. Trude, J., Kilsdonk, B., Grow, T. & Ott, B. The structure and tectonics of the Guyana Basin. *Geol. Soc. Lond. Spec. Publ.* **524**, 367–386 (2023).
5. Pindell, J. & Heyn, T. Dynamo-thermal subsidence and sag–salt section deposition as magma-rich rifted margins move off plume centres along incipient lines of break-up. *J. Geol. Soc.* **179**, jgs2021–jgs2095 (2022).
6. Reuber, K. R., Pindell, J. & Horn, B. W. Demerara Rise, offshore Suriname: Magma-rich segment of the Central Atlantic Ocean, and conjugate to the Bahamas hot spot. *Interpretation* **4**, T141–T155 (2016).
7. Basile, C. et al. Initiation of transform continental margins: the Cretaceous margins of the Demerara plateau. *Geol. Soc. Lond. Spec. Publ.* **524**, 327–337 (2023).
8. Pindell, J. L. Alleghenian reconstruction and subsequent evolution of the Gulf of Mexico, Bahamas, and Proto-Caribbean. *Tectonics* **4**, 1–39 (1985).
9. Gillard, M. et al. Tectonomagmatic evolution of the final stages of rifting along the deep conjugate Australian–Antarctic magma-poor rifted margins: Constraints from seismic observations: Australian–Antarctic margins evolution. *Tectonics* **34**, 753–783 (2015).
10. Gillard, M. et al. Birth of an oceanic spreading center at a magma-poor rift system. *Sci. Rep.* **7**, 15072 (2017).
11. Luyendyk, B. P. & Macdonald, K. C. Spreading center terms and concepts. *Geology* **4**, 369 (1976).
12. McClinton, J. T. & White, S. M. Emplacement of submarine lava flow fields: A geomorphological model from the Niños eruption at the Galápagos Spreading Center. *Geochem. Geophys. Geosyst.* **16**, 899–911 (2015).
13. Gao, D., Hurst, S., Karson, J., Delaney, J. & Spiess, F. Computer-aided interpretation of side-looking sonar images from the eastern intersection of the Mid-Atlantic Ridge with the Kane Transform. *J. Geophys. Res.* **103**, 20,997–21,014 (1998).
14. Dick, H. J. B., Lin, J. & Schouten, H. An ultraslow-spreading class of ocean ridge. *Nature* **426**, 405–412 (2003).

15. Yu, Z. et al. Distribution of large-scale detachment faults on mid-ocean ridges in relation to spreading rates. *Acta Oceanol. Sin.* **32**, 109–117 (2013).
16. Dannowski, A., Morgan, J. P., Grevemeyer, I. & Ranero, C. R. Enhanced mantle upwelling/melting caused segment propagation, oceanic core complex die off, and the death of a transform fault: the mid-Atlantic ridge at 21.5°N. *J. Geophys. Res. Solid Earth* **123**, 941–956 (2018).
17. Grevemeyer, I., Rüpke, L. H., Morgan, J. P., Iyer, K. & Devey, C. W. Extensional tectonics and two-stage crustal accretion at oceanic transform faults. *Nature* **591**, 402–407 (2021).
18. Schierjott, J. C. et al. How transform fault shear influences where detachment faults form near mid-ocean ridges. *Sci. Rep.* **13**, 9259 (2023).
19. Cannat, M. et al. Modes of seafloor generation at a melt-poor ultraslow-spreading ridge. *Geology* **34**, 605 (2006).
20. Harkin, C., Kuszniir, N., Tugend, J., Manatschal, G. & McDermott, K. Evaluating magmatic additions at a magma-poor rifted margin: An East Indian case study. *Geophys. J. Int.* <https://doi.org/10.1093/gji/ggz007> (2019).
21. Cannat, M. et al. On spreading modes and magma supply at slow and ultraslow mid-ocean ridges. *Earth Planet. Sci. Lett.* **519**, 223–233 (2019).
22. Tucholke, B. E. & Lin, J. A geological model for the structure of ridge segments in slow spreading ocean crust. *J. Geophys. Res. Solid Earth* **99**, 11937–11958 (1994).
23. Macdonald, K. C. Mid-ocean Ridge Tectonics, Volcanism And Geomorphology. in *Encyclopedia of Ocean Sciences 1798–1813* (Elsevier, 2001). <https://doi.org/10.1006/rwos.2001.0094>.
24. Manatschal, G. New models for evolution of magma-poor rifted margins based on a review of data and concepts from West Iberia and the Alps. *Int. J. Earth Sci.* **93**, 432–466 (2004).
25. Stica, J. M., Zalán, P. V. & Ferrari, A. L. The evolution of rifting on the volcanic margin of the Pelotas Basin and the contextualization of the Paraná–Etendeka LIP in the separation of Gondwana in the South Atlantic. *Mar. Pet. Geol.* **50**, 1–21 (2014).
26. Sauter, D. et al. Continuous exhumation of mantle-derived rocks at the Southwest Indian Ridge for 11 million years. *Nat. Geosci.* **6**, 314–320 (2013).
27. Lutz, R. et al. Evidence for mantle exhumation since the early evolution of the slow-spreading Gakkel Ridge, Arctic Ocean. *J. Geodyn.* **118**, 154–165 (2018).
28. Tugend, J. et al. Reappraisal of the magma-rich versus magma-poor rifted margin archetypes. *Geol. Soc. Lond. Spec. Publ.* **476**, 23–47 (2020).
29. Planke, S. & Eldholm, O. Seismic response and construction of seaward dipping wedges of flood basalts: Vøring volcanic margin. *J. Geophys. Res. Solid Earth* **99**, 9263–9278 (1994).
30. Paton, D. A., Pindell, J., McDermott, K., Bellingham, P. & Horn, B. Evolution of seaward-dipping reflectors at the onset of oceanic crust formation at volcanic passive margins: Insights from the South Atlantic. *Geology* **45**, 439–442 (2017).
31. Tomasi, S., Kuszniir, N., Manatschal, G. & Despinois, F. The challenge in restoring magma-rich rifted margins: The example of the Mozambique–Antarctica conjugate margins. *Gondwana Res* **95**, 29–44 (2021).
32. Whitmarsh, R. B., Manatschal, G. & Minshull, T. A. Evolution of magma-poor continental margins from rifting to seafloor spreading. *Nature* **413**, 150–154 (2001).
33. Mohn, G., Karner, G. D., Manatschal, G. & Johnson, C. A. Structural and stratigraphic evolution of the Iberia–Newfoundland hyper-extended rifted margin: a quantitative modelling approach. *Geol. Soc. Lond. Spec. Publ.* **413**, 53–89 (2015).
34. Lavier, L. L. & Manatschal, G. A mechanism to thin the continental lithosphere at magma-poor margins. *Nature* **440**, 324–328 (2006).
35. editors, O. G. J. ExxonMobil makes two new oil discoveries offshore Guyana. *Oil & Gas Journal* <https://www.ogj.com/exploration-development/discoveries/article/14284772/exxonmobil-makes-two-new-oil-discoveries-offshore-guyana> (2022).
36. Pindell, J., Graham, R. & Horn, B. W. Role of outer marginal collapse on salt deposition in the eastern Gulf of Mexico, Campos and Santos basins. *Geol. Soc. Lond. Spec. Publ.* **476**, 317–331 (2020).
37. Pindell, J., Villagómez, D., Molina-Garza, R., Graham, R. & Weber, B. A revised synthesis of the rift and drift history of the Gulf of Mexico and surrounding regions in the light of improved age dating of the Middle Jurassic salt. *Geol. Soc. Lond. Spec. Publ.* **504**, 29–76 (2021).
38. Dick, H., Natland, J. & Ildefonse, B. Past and future impact of deep drilling in the oceanic crust and mantle. *Oceanography* **19**, 72–80 (2006).
39. Peron-Pinvidic, G., Manatschal, G. & Osmundsen, P. T. Structural comparison of archetypal Atlantic rifted margins: A review of observations and concepts. *Mar. Pet. Geol.* **43**, 21–47 (2013).
40. McDermott, K., Gillbard, E. & Clarke, N. From Basalt to Skeletons – the 200 million-year history of the Namibian margin uncovered by new seismic data. *First Break* **33**, 77–85 (2015).
41. Geoffroy, L., Chauvet, F. & Ringenbach, J.-C. Middle-lower continental crust exhumed at the distal edges of volcanic passive margins. *Commun. Earth Environ.* **3**, 95 (2022).
42. Greenroyd, C. J., Peirce, C., Rodger, M., Watts, A. B. & Hobbs, R. W. Demerara Plateau - the structure and evolution of a transform passive margin. *Geophys. J. Int.* **172**, 549–564 (2008).
43. Bird, D. E., Hall, S. A., Burke, K., Casey, J. F. & Sawyer, D. S. Early Central Atlantic Ocean seafloor spreading history. *Geosphere* **3**, 282 (2007).
44. Geoffroy, L., Gernigon, L. & Foulger, G. R. Linear magnetic anomalies and the limits of oceanic crust in oceans. in G. R. Foulger et al. (Eds.), *In the footsteps of Warren B. Hamilton: New Ideas in Earth Science. Geol. Soc. Am. Spec. Pap.* **553**, 1–14 (2021). [https://doi.org/10.1130/2021.2553\(06\)](https://doi.org/10.1130/2021.2553(06)).
45. Spector, A. & Grant, F. S. Statistical models for interpreting aeromagnetic data. *Geophysics* **35**, 293–302 (1970).
46. Gradstein, F. M. & Ogg, J. G. The Chronostratigraphic Scale. in *Geologic Time Scale 2020* 21–32 (Elsevier, 2020). <https://doi.org/10.1016/B978-0-12-824360-2.00002-4>.
47. Tominaga, M., Tivey, M. A. & Sager, W. W. A New Middle to Late Jurassic Geomagnetic Polarity Time Scale (GPTS) From a Multiscale Marine Magnetic Anomaly Survey of the Pacific Jurassic Quiet Zone. *J. Geophys. Res. Solid Earth* **126**, <https://doi.org/10.1029/2020JB021136> (2021).
48. Lawver, L. A., Norton, I. O., Dalziel, I. W. D. & Davis, M. D. *The Plates 2020 Atlas of Plate Reconstructions (500Ma to Present Day)*, *Plates Progress Report No. 396-1220*, University of Texas Institute for Geophysics Technical Report no. 238. (University of Texas Institute for Geophysics).
49. Müller, R. D., Sdrolias, M., Gaina, C. & Roest, W. R. Age, spreading rates, and spreading asymmetry of the world's ocean crust: Digital models of the world's ocean crust. *Geochem. Geophys. Geosystems* **9**, n/a–n/a (2008).
50. Hesselbo, S. P., Ogg, J. G., Ruhl, M., Hinnov, L. A. & Huang, C. J. The Jurassic Period. In *Geologic Time Scale 2020* 955–1021 (Elsevier, 2020). <https://doi.org/10.1016/B978-0-12-824360-2.00026-7>.
51. Davis, J. K., Bécél, A. & Buck, W. R. Estimating emplacement rates for seaward-dipping reflectors associated with the U.S. East Coast Magnetic Anomaly. *Geophys. J. Int.* **215**, 1594–1603 (2018).
52. Toft, P. B., Arkani-Hamed, J. & Haggerty, S. E. The effects of serpentinization on density and magnetic susceptibility: a petrophysical model. *Phys. Earth Planet. Inter.* **65**, 137–157 (1990).
53. Carlson, R. L., Snow, K. R. & Wilkins, R. H. Density of old oceanic crust: an estimate derived from downhole logging on ODP LEG 102., *Proc. Ocean Drill. Program, Sci. Results* **102**, 63–68 (1988).

54. Dick, H. J. B. et al. A long in situ section of the lower ocean crust: results of ODP Leg 176 drilling at the Southwest Indian Ridge. *Earth Planet. Sci. Lett.* **179**, 31–51 (2000).
55. Kneller, E. A., Johnson, C. A., Kamer, G. D., Einhorn, J. & Queffelec, T. A. Inverse methods for modeling non-rigid plate kinematics: Application to mesozoic plate reconstructions of the Central Atlantic. *Comput. Geosci.* **49**, 217–230 (2012).
56. Pindell, J. L. & Kennan, L. Tectonic evolution of the Gulf of Mexico, Caribbean and northern South America in the mantle reference frame: an update. *Geol. Soc. Lond. Spec. Publ.* **328**, 1–55 (2009).
57. Rouméjon, S. & Cannat, M. Serpentinization of mantle-derived peridotites at mid-ocean ridges: Mesh texture development in the context of tectonic exhumation. *Geochem. Geophys. Geosystems* **15**, 2354–2379 (2014).
58. Gillard, M. et al. The role of serpentinization and magmatism in the formation of decoupling interfaces at magma-poor rifted margins. *Earth-Sci. Rev.* **196**, 102882 (2019).
59. Epin, M.-E. et al. Polyphase tectono-magmatic evolution during mantle exhumation in an ultra-distal, magma-poor rift domain: example of the fossil Plattia ophiolite, SE Switzerland. *Int. J. Earth Sci.* **108**, 2443–2467 (2019).
60. Basile, C. Transform continental margins — part 1: Concepts and models. *Tectonophysics* **661**, 1–10 (2015).
61. Vine, F. J. & Moores, E. M. A Model for the Gross Structure, Petrology, and Magnetic Properties of Oceanic Crust. in *Earth and Space Sciences: A Memoir in Honor of Hary Hammond Hess* 195–205 (1972).
62. Franke, D. Rifting, lithosphere breakup and volcanism: Comparison of magma-poor and volcanic rifted margins. *Mar. Pet. Geol.* **43**, 63–87 (2013).
63. Kamer, G. D. et al. Chapter 9: Tectono-Magmatic Development of the Santos and Campos Basins, Offshore Brazil. in *Memoir 124: The Supergiant Lower Cretaceous Pre-Salt Petroleum Systems of the Santos Basin, Brazil* (eds. Mello, M. R., Yilmaz, P. O. & Katz, B. J.) 215–256 (AAPG, 2021). <https://doi.org/10.1306/13722321MSB.9.1853>.
64. Canales, J. P., Collins, J. A., Escartín, J. & Detrick, R. S. Seismic structure across the rift valley of the Mid-Atlantic Ridge at 23°20' (MARK area): Implications for crustal accretion processes at slow spreading ridges. *J. Geophys. Res. Solid Earth* **105**, 28411–28425 (2000).
65. GEBCO Bathymetric Compilation Group 2020. The GEBCO_2020 Grid - a continuous terrain model of the global oceans and land. (2020) <https://doi.org/10.5285/A29C5465-B138-234D-E053-6C86ABC040B9>.
66. Tozer, B. et al. Global Bathymetry and Topography at 15 Arc Sec: SRTM15+. *Earth Space Sci* **6**, 1847–1864 (2019).
67. Schettino, A. & Scotese, C. R. Apparent polar wander paths for the major continents (200 Ma to the present day): a palaeomagnetic reference frame for global plate tectonic reconstructions. *Geophys. J. Int.* **163**, 727–759 (2005).

Acknowledgements

We acknowledge Hess Corporation for the time, resources, funding, and permission to both work on and publish this paper. We thank the partners, GGMC, PGS ION, and CGG for high-quality seismic data and for granting permission to publish. We thank reviewers James Pindell and Dengliang Gao

for careful, useful, and professional critiques of the original and revised manuscripts. Their insights improved this contribution immeasurably. We also acknowledge a third anonymous reviewer. We thank Frank Peel both for informative conversations on Northern Atlantic margins and for instruction on illustrating the rate competition between extension and magma addition. Our Hess colleagues in the Guyana and Suriname Exploration teams contributed countless hours of interpretation, discussion, and good spirited argument on the development of the margin.

Author contributions

B.K.: project concept and organization, seismic interpretation, writing. J.T.: seismic interpretation and writing. T.G.: gravity and magnetic data analyses. B.O.: seismic interpretation. G.M.: guidance on crustal interpretation, tectonic evolution, observations, and analogues. All authors contributed to integrating data and analyses, formulating main points, and drafting the final manuscript.

Competing interests

The authors declare no competing interests.

Additional information

Supplementary information The online version contains supplementary material available at <https://doi.org/10.1038/s43247-024-01265-2>.

Correspondence and requests for materials should be addressed to Bill Kilsdonk.

Peer review information *Communications Earth & Environment* thanks Dengliang Gao and the other, anonymous, reviewer(s) for their contribution to the peer review of this work. Primary Handling Editors: Joe Aslin and Carolina Ortiz Guerrero. A peer review file is available.

Reprints and permissions information is available at <http://www.nature.com/reprints>

Publisher's note Springer Nature remains neutral with regard to jurisdictional claims in published maps and institutional affiliations.

Open Access This article is licensed under a Creative Commons Attribution 4.0 International License, which permits use, sharing, adaptation, distribution and reproduction in any medium or format, as long as you give appropriate credit to the original author(s) and the source, provide a link to the Creative Commons licence, and indicate if changes were made. The images or other third party material in this article are included in the article's Creative Commons licence, unless indicated otherwise in a credit line to the material. If material is not included in the article's Creative Commons licence and your intended use is not permitted by statutory regulation or exceeds the permitted use, you will need to obtain permission directly from the copyright holder. To view a copy of this licence, visit <http://creativecommons.org/licenses/by/4.0/>.

© The Author(s) 2024